Probing the Active Center of Benzaldehyde Lyase with Substitutions and the Pseudosubstrate Analogue Benzoylphosphonic Acid Methyl Ester†

Gabriel S. Brandt,‡ Natalia Nemeria,§ Sumit Chakraborty,§ Michael J. McLeish,|| Alejandra Yep,|| George L. Kenyon,|| Gregory A. Petsko,‡ Frank Jordan,*,§ and Dagmar Ringe*,‡

Department of Biochemistry, Brandeis University, Waltham, Massachusetts 02454, Department of Chemistry, Rutgers University, Newark, New Jersey 07102, and Department of Medicinal Chemistry, College of Pharmacy, University of Michigan, Ann Arbor, Michigan 48109

Received March 14, 2008; Revised Manuscript Received May 22, 2008

ABSTRACT: Benzaldehyde lyase (BAL) catalyzes the reversible cleavage of (*R*)-benzoin to benzaldehyde utilizing thiamin diphosphate and Mg^{2+} as cofactors. The enzyme is important for the chemoenzymatic synthesis of a wide range of compounds via its carboligation reaction mechanism. In addition to its principal functions, BAL can slowly decarboxylate aromatic amino acids such as benzoylformic acid. It is also intriguing mechanistically due to the paucity of acid−base residues at the active center that can participate in proton transfer steps thought to be necessary for these types of reactions. Here methyl benzoylphosphonate, an excellent electrostatic analogue of benzoylformic acid, is used to probe the mechanism of benzaldehyde lyase. The structure of benzaldehyde lyase in its covalent complex with methyl benzoylphosphonate was determined to 2.49 Å (Protein Data Bank entry 3D7K) and represents the first structure of this enzyme with a compound bound in the active site. No large structural reorganization was detected compared to the complex of the enzyme with thiamin diphosphate. The configuration of the predecarboxylation thiamin-bound intermediate was clarified by the structure. Both spectroscopic and X-ray structural studies are consistent with inhibition resulting from the binding of MBP to the thiamin diphosphate in the active centers. We also delineated the role of His29 (the sole potential acid−base catalyst in the active site other than the highly conserved Glu50) and Trp163 in cofactor activation and catalysis by benzaldehyde lyase.

Benzaldehyde lyase (BAL,[1] EC 4.1.2.38) is a thiamin diphosphate (ThDP)-dependent enzyme, which carries out the reversible conversion of (*R*)-benzoin to benzaldehyde (eq 1). The enzyme is a valuable tool in chemoenzymatic synthesis

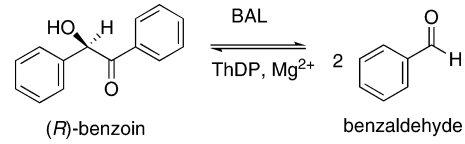

of chiral α-hydroxyketones (*1, 2*). In addition to its lyase and carboligase activity, BAL is now clearly documented to have slow decarboxylase activity with benzoylformate, producing (*R*)-benzoin as a product and proceeding via the enamine intermediate (*3*). A plausible mechanism for the reactions carried out by BAL (Scheme 1) starts with a nucleophilic attack at the carbonyl carbon of benzoin by the ThDP ylide producing the first covalent intermediate C2-(α,*β*-dihydroxy-α,*β*-diphenyl)ethylThDP (DDEThDP). DDEThDP releases the first molecule of benzaldehyde producing the enamine, which undergoes C2α protonation to form C2α-hydroxybenzylThDP (HBThDP). A second molecule of benzaldehyde is then released, and the ThDP ylide is regenerated (Scheme 1).

In the past, substrate analogues, including sodium methyl acetylphosphonate, sodium acetylphosphinate, and sodium acetylmethylphosphinate, have been found to be efficiently converted to the first covalent intermediate by a number of ThDP enzymes (*4–7*). By virtue of a C−P bond rather than a C−C bond, this intermediate, an analogue of C2α-lactylthiamin diphosphate (LThDP), the pyruvate−ThDP adduct, is stable. Taking advantage of the decarboxylase

† Supported by NIH Grant NRSA F32GM069057 (G.S.B.), NIH Grant GM050380 (Rutgers University), and NSF Grant EF-0425719 (Brandeis University and University of Michigan). Use of the Advanced Photon Source was supported by the U.S. Department of Energy, Basic Energy Sciences, and Office of Science, under Contract No. W-31-109-Eng-38. Use of BioCARS Sector 14 was supported by the National Institutes of Health, National Center for Research Resources, under Grant No. RR007707.

* To whom correspondence should be addressed. D.R.: e-mail, ringe@brandeis.edu; telephone, (781) 736-4902; fax, (781) 736-2405. F.J.: e-mail, frjordan@newark.rutgers.edu; telephone, (973) 353-5470; fax, (973) 353-1264.

‡ Brandeis University.

§ Rutgers University.

|| University of Michigan.

[1] Abbreviations: ThDP, thiamin diphosphate; MThDP, C2α-mandelylThDP, the covalent adduct formed between ThDP and benzoylformate; HBThDP, C2α-hydroxybenzylThDP, the covalent adduct formed between ThDP and the product of the reaction benzaldehyde; LThDP, covalent adduct formed between ThDP and pyruvate; BAL, benzaldehyde lyase; MBP, methyl benzoylphosphonate sodium salt; BFDC, benzoylformate decarboxylase; DDEThDP, C2-(α,*β*-dihydroxy-α,*β*-diphenyl)ethylThDP; PMThDP, C2α-phosphonomandelyl thiamin diphosphate methyl ester; YPDC, pyruvate decarboxylase from the yeast *Saccharomyces cerevisiae*; POX, pyruvate oxidase from *Lactobacillus plantarum*; E1ec, first component of the *Escherichia coli* pyruvate dehydrogenase complex; E1h, first component of the human pyruvate dehydrogenase complex; SVD, single-value decomposition; CD, circular dichroism; wt, wild-type BAL.

10.1021/bi8004413 CCC: $40.75
Published on Web 06/21/2008

Scheme 1: Proposed Mechanism of Reversible Benzoin Condensation in BAL with the Benzoylformate Decarboxylase Colored Blue

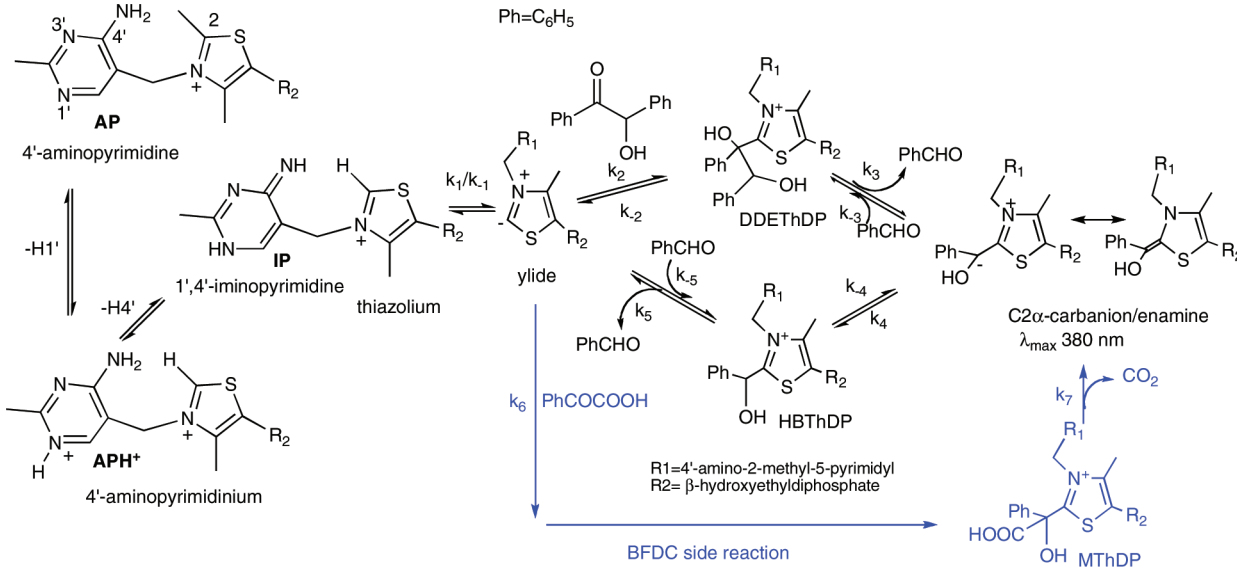

activity found in BAL with benzoylformate, we have examined the interaction of this enzyme with benzoylphosphonic acid methyl ester [MBP (Figure 1)]. It was thought that MBP would behave as an analogue of benzoylformate,

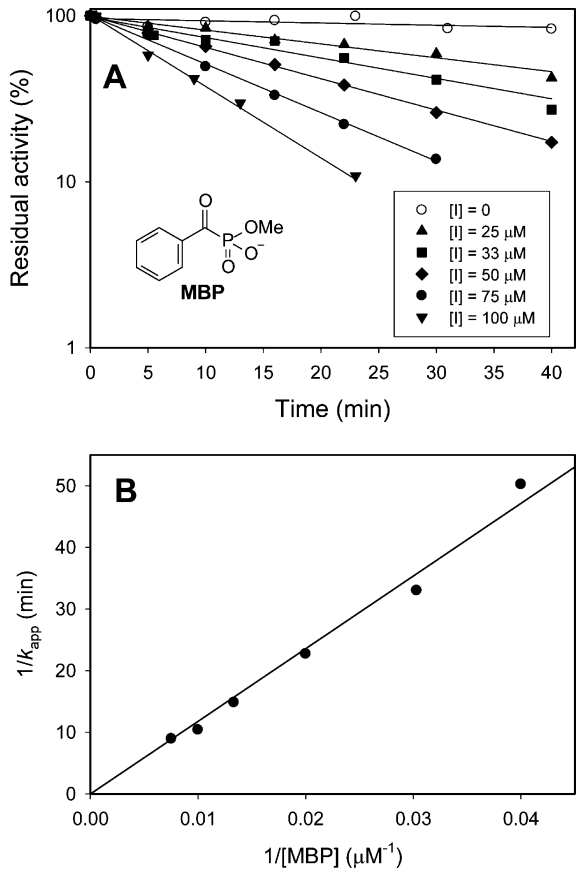

FIGURE 1: (A) Time- and concentration-dependent inactivation of BAL by MBP. The structure of MBP is inset. (B) Reciprocal (Kitz and Wilson) plot of $1/k_{inact,observed}$ vs 1/[MBP]. BAL (40 μg/mL, 0.68 μM active centers) in 50 mM Tris-HCl (pH 8.0) containing 1 mM $MgSO_4$ and 0.5 mM ThDP was incubated with MBP (25−100 μM) at 30 °C. At appropriate time intervals, aliquots (10 μL) were withdrawn and diluted 1:100 into a standard assay mixture containing 1 mM benzoin.

onto which ThDP adds at the keto carbon in an enzyme-catalyzed reaction to form a C2α-phosphonomandelylThDP methyl ester [PMThDP (Scheme 2)]. The latter is unable to undergo dephosphonylation and would presumably form a stable predecarboxylation analogue of C2α-mandelylThDP (MThDP), the first covalent ThDP-bound intermediate in the decarboxylation of benzoylformate. In doing so, MBP might provide insight into the formation of intermediates with tetrahedral substitution at the C2α atom, including the state of ionization and tautomeric nature of the 4′-aminopyrimidine ring of ThDP on BAL, a major current focus of research of the Rutgers group with several collaborators (*4–6, 8–12*). We have now demonstrated in a number of ThDP-dependent enzymes that the 4′-aminopyrimidine ring of ThDP actively participates and plays a very crucial role in catalysis via its 1′,4′-iminopyrimidine tautomeric form (*4–7*).

We show kinetically and spectroscopically that the stable intermediate indeed forms and determine the structure of benzaldehyde lyase in its covalent complex with MBP to 2.49 Å [Protein Data Bank (PDB) entry 3D7K]. This represents the first structure of BAL with a substrate analogue bound. No large structural reorganization was detected in this complex when compared to the complex of BAL with ThDP alone (*13, 14*). The crystal structure of the BAL complex reveals the presence of only two residues with side chains within 4 Å of the ThDP that are capable of proton transfer. The first is Glu50, a nearly universally conserved feature of thiamin enzymes, which is located within hydrogen bonding distance of the N1′ atom of the 4′-aminopyrimidine ring, and it is presumed to participate in the acid−base chemistry leading to the 1′,4′-iminopyrimidine tautomeric form of the coenzyme. The second is His29, which is hydrogen bonded to a water molecule 3.6 Å from C2 of the thiazolium ring but too far from the N4′ atom to have any direct interaction with it. Modeling of DDEThDP into the active site of BAL led to the suggestion that the side chain of His29 has a role in deprotonating the "distal" OH group of the bound benzoin, triggering release of the first benzaldehyde molecule thus forming the enamine. Initial site-directed mutagenesis studies found that the H29A variant

Scheme 2: Mechanism of Formation of MThDP and PMThDP

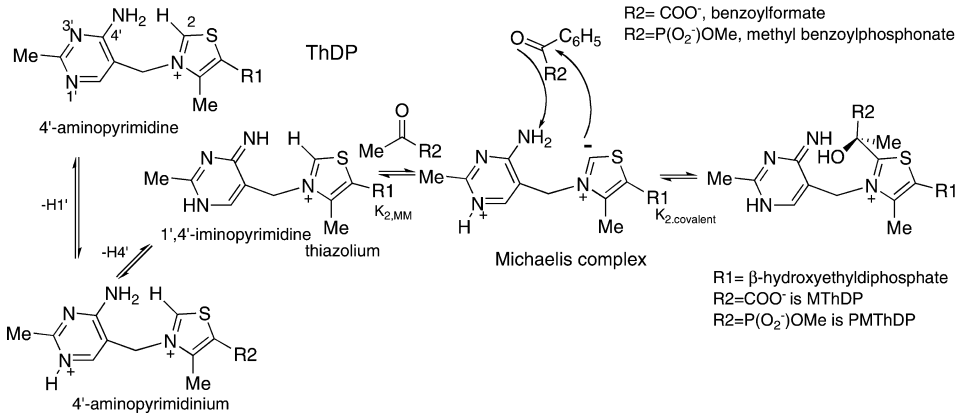

exhibited some reduction in activity, albeit a reduction apparently too small in magnitude for the residue to be participating in critical acid−base activity (*15*). We here further delineate the role of His29 and another active site residue, Trp163, in catalysis by BAL.

MATERIALS AND METHODS

Synthesis of Methyl Benzoylphosphonate. MBP was synthesized according to the method of Karaman, with some modifications (*16*). Briefly, dimethyl benzoylphosphonate was prepared by dropwise addition of 4.75 mL of trimethylphosphite (5 g, 40.3 mmol) to 4.68 mL benzoyl chloride (5.66 g, 40.3 mmol) under nitrogen at 0 °C. After the addition was complete, the reaction mixture was stirred at 0 °C for 30 min and then allowed to warm to room temperature over a period of 3 h. The resulting yellowish oil was collected by vacuum distillation after a small forerun to yield 7.55 g (87%, lit. 89%): ^{1}H NMR (500 MHz, $CDCl_3$, 0.5% TMS) δ 8.253 (d, J = 7.5 Hz, 2H), 7.652 (t, J = 7.5 Hz, 1H), 7.519 (t, J = 7.5 Hz, 2H), 3.922 (d, J = 10.5 Hz, 6H). A portion of the dimethyl benzoylphosphonate product (1 g, 4.67 mmol) was added to a solution of 2.1 g (14.01 mmol) of dry sodium iodide in 25 mL of dry acetone under nitrogen, at 25 °C. After being stirred overnight, the reaction mixture was evaporated to dryness. The solid mixture was triturated several times with ethyl acetate and the solvent evaporated to dryness. The crude product was recrystallized from absolute ethanol to yield 0.82 g (79%, lit. 98%): ^{1}H NMR (500 MHz, D_2O-DSS) δ 8.202 (d, J = 7.5 Hz, 2H), 7.748 (t, J = 7.5 Hz, 1H), 7.612 (t, J = 7.5 Hz, 2H), 3.695 (d, J = 5.5 Hz, 3H).

Bacteria and Plasmids. Plasmids pKKBAL-His, pKKBALH29A-His, and pKKBALW163A-His were used for expression and purification of BAL and its H29A and W163A variants. The construction of H29A BAL was reported previously (*15*). For the construction of W163A BAL, site-directed mutagenesis was performed according to the QuikChange protocol using *Pfu* polymerase (Invitrogen) and pKKBAL-His (*3*) as a template. The forward primer used for mutagenesis was as follows with the mutated codon underlined and lowercase letters indicating a base change from the wild type: 5′-GTGTTGCTGGATCTGCCGgcG-GATATcCTGATGAACCAG-3′. The additional silent mutation was introduced to generate a new restriction site for EcoRV, which was used for the initial screening of the mutation by restriction analysis. The resulting plasmid was sequenced to ensure that only the intended mutation had occurred.

Expression and Purification of BAL and Its Variants. Plasmids pKKBAL-His, pKKBALH29A-His, and pKKBALW163A-His were transformed into BL21(DE3)pLysS cells (Novagen). Expression and purification were carried out essentially as described previously (*15*). The fractions with the highest purity as assessed by SDS−PAGE were pooled, and the buffer was exchanged for storage buffer [50 mM potassium phosphate buffer (pH 6.5), 1 mM $MgSO_4$, 0.5 mM ThDP, and 10% glycerol] using Econo-Pac 10 DG desalting columns (Bio-Rad). The protein samples were concentrated with Amicon Ultra centrifugal filters (Millipore) and stored at −80 °C. The enzyme preparations were apparently homogeneous as judged by SDS−PAGE. Protein concentrations were determined with the Bradford assay using bovine serum albumin as a standard.

Activity and Related Measurements. The activity of BAL and its variants was measured in 1 mL of 50 mM Tris-HCl buffer (pH 8.0) containing 1 mg/mL bovine serum albumin, 1 mM $MgSO_4$, 0.50 mM ThDP, 0.25 unit of horse liver alcohol dehydrogenase (HLADH; 12.5 units/mL stock solution), 0.60 mM benzoin (0.01 M stock of benzoin was made in 99.9% DMSO), and 0.35 mM NADH. The reaction was initiated by the addition of 0.5 μg of BAL and was followed for 5 min at 340 nm and 30 °C. The activity of BAL was approximately 30−40 units/mg of protein.

Circular Dichroism. CD studies were performed on a Chirascan CD spectrometer from Applied Photophysics (Leatherhead, United Kingdom) in a 1 cm path length cell in the near-UV region (as specified in each figure) at 30 °C unless otherwise specified. To the BAL (2 mg/mL, concentration of active centers of 33.9 μM or as described in the figure legends) in 50 mM Tris-HCl (pH 8.0) containing ThDP (150−200 μM) and $MgSO_4$ (1 mM) was added 1−500 μM MBP. To check for reversibility of inhibition by substrate analogues, the BAL titrated with a substrate analogue was dialyzed overnight against 2 L of 50 mM Tris-HCl (pH 8.0) and the CD spectra were recorded.

Time-Resolved CD. Stopped-flow circular dichroism experiments were carried out on a π*-180 CDF spectrometer from Applied Photophysics using a slit width of 2 mm and a path length of 10 mm. The temperature was maintained at 30 °C. In a typical experiment, the required amount of BAL in buffer A, containing 50 mM Tris-HCl (pH 8.0), 1 mM

ThDP, 2.5 mM $MgSO_4$, and 10% (v/v) DMSO (the DMSO is needed to keep the solutions homogeneous), was mixed with an equal volume of substrate at the intended concentration in the same buffer. The reactions were monitored for various amounts of time (0.01−200 s), and data points were collected at varied time intervals (2.5−10 ms). The data were analyzed using Pro-K Global Analysis. Single-value decompositions (SVDs) were determined where necessary. SigmaPlot 2001 version 7.101 was used for all data analysis.

Protein Crystallization. For cocrystallization of BAL with MBP, the procedure of Mosbacher et al. for wild-type BAL crystallization by vapor diffusion was followed closely (*14*). Briefly, BAL was dialyzed and then concentrated to 11 mg/mL (0.19 mM) in a solution of 5 mM HEPES (pH 6.9) also containing 10 mM NaCl, 2 mM $MgCl_2$, 2 mM DTT, and 0.2 mM ThDP. Aliquots of the protein solution were flash-frozen in liquid nitrogen and stored at −80 °C. A well solution of 100 mM MES (pH 6.9) and 50% (v/v) PEG 200 was prepared. A stock solution of MBP was prepared at a concentration of 1 M in DMSO and likewise stored at −80 °C. In preparation for cocrystallization, the MBP solution was thawed and diluted 1:10 into the protein storage buffer. Typically, 0.2 μL of MBP was incubated with 10 μL of the protein solution to give 10.8 mg/mL (0.19 mM) protein, 2 mM MBP, and 0.2% (v/v) DMSO. Subsequent to this incubation, the BAL−MBP solution was combined with well solution at a ratio of 1:1. The Mosbacher procedure makes use of a low-melting agarose solution as an additive (*14*). In our hands, no significant difference in crystallization rate, crystal appearance, or extent of diffraction was observed with the addition of agarose. Hundreds of small rodlike crystals typically appeared within 24 h, many with a characteristic notch at each end. Larger crystals were typically obtained with the BAL−MBP complexes than with BAL alone, although the quality of diffraction was not significantly improved. Crystals were flash-frozen in liquid nitrogen without the use of additional cryoprotectant.

X-ray Data Collection. Crystals were irradiated at beamline 14-ID administered by BioCARS (Advanced Photon Source, Argonne National Laboratory, Argonne, IL). Data reduction and processing were carried out using the HKL 2000 software package and the CCP4 suite of programs (*17, 18*). A single monomer of the BAL crystal structure of Mosbacher (PDB entry 2AG0) was used as a search model for molecular replacement in Molrep (*19*) and Phaser (*20*). The unit cell of the BAL−MBP cocrystal was similar to that of BAL alone, but only half as long in its longest dimension. To obtain a molecular replacement solution, we were forced to scale the data in the $P3_221$ space group, the enantiomorph of the space group of BAL alone. The asymmetric unit was found to consist of a single dimer. Subsequent refinement of the data was carried out using the CCP4 software suite. Crystallographic data and refinement statistics are given in Table 1, and the structure has been identified as PDB entry 3D7K.

Structural Refinement. Subsequent to molecular replacement, the initial model was refined using Refmac (*21*). Water molecules were added in an automated fashion into difference density peaks with an intensity greater than 3σ, using Coot (*22*). Given the spatial resolution, the additional criteria of spherical shape, the presence of at least one hydrogen bonding partner, and a location outside the active site were checked by hand and utilized in assigning water molecules to difference density (*23, 24*). After refinement with a model including these water molecules, the ThDP cofactors were manually placed, using Coot, into the positive difference density and further positioned by real-space refinement. After refinement in the presence of polypeptide, water and cofactors, omit maps were generated and the ligand was placed by an analogous process. Coordinate files and appropriate restraints for the ThDP−MBP reaction product were generated using the Sketcher program of the CCP4 suite (*25*) and the PRODRG server (*26*). These restraints were retained for the ligand throughout refinement. After the cofactors and ligand were refined, active site waters were assigned to spherical regions of difference density greater than 4σ. A number of regions were observed to be disordered in the final structure and are listed in Table 1. The final structural solution was subjected to validation using SFCheck, ProCheck, and WhatCheck (*27–29*).

Table 1: Data, Model, and Crystallographic Statistics for the BAL Structure with MBP

PDB entry	3D7K
beamline	APS, BioCARS, 14-ID
wavelength (Å)	0.97934
space group	$P3_221$
unit cell dimensions	$a = b = 152$ Å, $c = 98$ Å
resolution limits	46.0−2.49 (2.59−2.49)[a]
total no. of reflections	375040
no. of unique reflections	43108
completeness (%) (last shell)	93.7 (79.3)[a]
redundancy (last shell)	8.7 (3.9)[a]
$I/\sigma(I)$	14.4 (1.4)[a]
R_{merge}	0.14 (0.67)[a]
unit cell contents	
no. of molecules per ASU	2
solvent content (%)	55.3
refinement statistics	
resolution range (Å)	46.0−2.49
R_{work} (%)	19.5
R_{free} (%)	24.9
no. of residues	1110
no. of waters	186
average B factor (Å^2)	42
root-mean-square deviation	
bond lengths (Å)	0.02
bond angles (deg)	2.3
Ramachandran analysis	
most favored (%)	86.4
allowed (%)	13.1
disordered regions	A265−268, A290−291, A367−369, A553−555, B265−266

[a] Values in parentheses are for the highest-resolution shell unless otherwise indicated.

RESULTS

MBP Binds in the Active Center of Benzaldehyde Lyase. Kinetics of Inhibition of BAL by MBP. We have shown previously that BAL can catalyze the decarboxylation of benzoylformate (*3*), and given that methyl benzoylphosphonate is an analogue of benzoylformate, we thought MBP may also react with BAL. Preliminary experiments, carried out in the presence of 100 μM benzoin (i.e., $\sim K_m$), showed that MBP had little effect until concentrations reached 1−2 mM, whereupon some curvature was noticed in the progress curves (data not shown). This curvature was indicative of time-dependent inactivation, presumably due to the formation of C2α-phosphonomandelylThDP (PMThDP). Accordingly, we

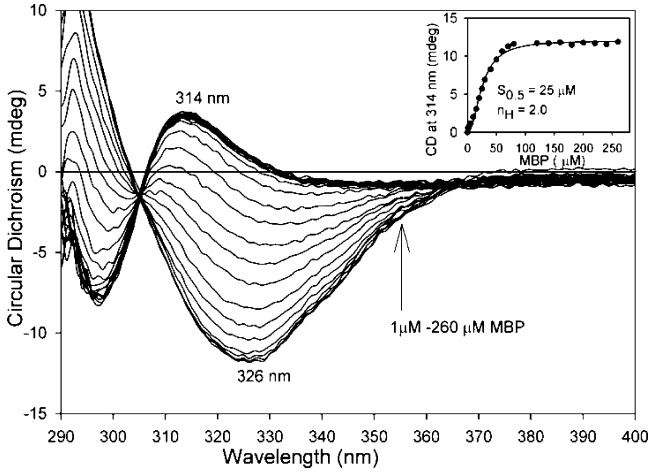

FIGURE 2: Near-UV CD spectra of BAL treated with MBP (inset). BAL (2.5 mg/mL, concentration of active centers of 41.67 μM) in 50 mM Tris-HCl (pH 8.0) containing 1 mM ThDP and 2.5 mM $MgSO_4$ was titrated with MBP (1−260 μM). The inset shows that the positive CD band at 314 nm reached the limiting value with a $K_{d,MBP}$ of 25 μM and an n_H of 2.0. The CD at 314 nm was obtained by the subtraction of the CD at 314 nm in the absence of MBP.

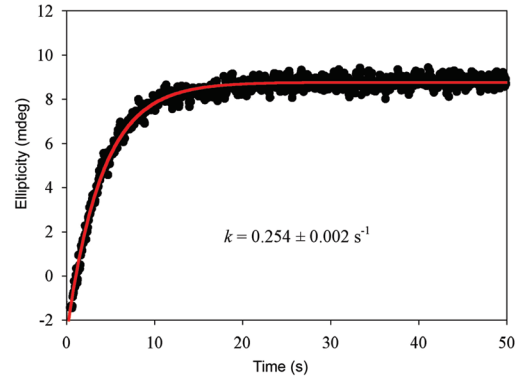

FIGURE 3: Rate of 1′,4′-iminoPMThDP formation from MBP by BAL using stopped-flow CD. BAL (2.0 mg/mL, concentration of active centers of 33.9 μM) in 50 mM Tris-HCl (pH 8.0), containing 1 mM ThDP, 2.5 mM $MgSO_4$, and 10% (v/v) DMSO, in one syringe was mixed with an equal volume of 1 mM MBP in the same buffer in the second syringe, and the reaction was monitored at 313 nm for 50 s at 30 °C as described in Materials and Methods. Data were fitted to a single-exponential rise to maximum.

carried out a dilution study in which BAL (40 μg/mL) was incubated with varying concentrations of MBP. At appropriate time intervals, aliquots were assayed in the presence of a saturating level of (*R*)-benzoin to determine the residual activity. The results, shown in Figure 1A, are clearly indicative of time- and concentration-dependent inhibition but do not show evidence of saturation. A double-reciprocal (Kitz−Wilson) replot of the data from Figure 1A is presented in Figure 1B. The straight line with a *y*-intercept approaching zero suggests that only a weak complex is formed between BAL and MBP (*30*) and that the inactivation is fast compared to the formation of the BAL−MBP complex. A plot of k_{obs} values versus MBP concentration (not shown) yielded a second-order rate constant of 885 M^{-1} min^{-1}.

Circular Dichroism Observation of the 1′,4′-Iminopyrimidine Form of a Covalent Intermediate on BAL Using Methyl Benzoylphosphonate. Next, we needed to ascertain whether the covalent intermediate that MBP forms with ThDP resembles the predecarboxylation intermediate MThDP. This would be apparent from the CD band at 300−314 nm which reflects our general finding that ThDP analogues with tetrahedral substitution at the C2α atom exist in their 1′,4′-iminopyrimidine tautomeric form.

The near-UV CD spectrum (Figure 2) of the BAL−ThDP complex exhibited the negative CD band at 326 nm which has been assigned to the 4′-aminopyrimidine (AP) form of ThDP bound to the enzyme (*5*). Upon addition of 1−260 μM MBP, the magnitude of this CD band was significantly reduced, and in its place a positive CD band at 312−314 nm developed and reached a limiting value ($S_{0.5\ MBP}$ = 25 μM; Hill coefficient n_H = 2.0) (Figure 2). On the basis of model spectroscopic studies and CD studies on six ThDP enzymes (*4–7, 9, 10, 31*), the CD band at 312−314 nm was assigned to the 1′,4′-iminopyrimidine (IP) form of the first covalent intermediate on BAL, PMThDP (Scheme 2). The CD maximum for the IP form was shifted from 299 nm on BFDC (to be published) to 312−314 nm in BAL, and this shift could be explained by the hydrophobic active centers of BAL, also supported by model studies at Rutgers (*12*).

The amplitude of the positive CD band at 314 nm was unchanged after overnight dialysis of a MBP−BAL complex. It was also shown that benzoin could regenerate activity when added to MBP-inhibited BAL, suggesting reversibility of MBP binding (data not shown).

The reaction between BAL (2 mg/mL, concentration of active centers of 33.94 μM) and 2 mM MBP was monitored by stopped-flow CD. A positive band at 313 nm developed and reached a maximum in approximately 10 s with a rate constant of 0.254 ± 0.002 s^{-1} for PMThDP formation (Figure 3).

The value of n_H of 2.0 (Figure 2 inset) indicates positive cooperativity of active centers on MBP binding (four active centers are suggested by the X-ray structure). An n_H of 1.42 (with an $S_{0.5}$ of 0.095 mM) was obtained from a steady-state kinetic experiment for the breakdown of (*R*)-benzoin to benzaldehyde, also indicating positive cooperativity of at least two active centers in BAL on substrate or substrate−analogue binding (*3*). Size-exclusion chromatographic experiments suggested a molecular mass of 216 kDa, consistent with a tetramer in solution (*32*), as also suggested by the X-ray structure of BAL (*14*).

Structural Characterization of BAL Cocrystallized with MBP. To confirm the structure of the product of the reaction between the enzyme and MBP, the structure of the complex was determined. BAL from *Pseudomonas fluorescens* is a 555-amino acid polypeptide that is tetrameric in solution (*32*). In complex with methyl benzoylphosphonate, the protein crystallizes in trigonal space group $P3_221$ with unit cell dimensions of 152 Å × 152 Å × 98 Å (Table 1). The asymmetric unit contains a dimer, rather than the dimer of dimers observed for the protein in the absence of MBP (*13, 14*). A crystallographic 2-fold axis recapitulates the tetrameric assembly seen in those structures. The substrate binding site is at the interface of the two subunits of the noncrystallographic dimer, and both binding sites are seen to be occupied in the crystal structure. Differences between the two binding sites represented in the asymmetric unit are slight, with a 0.2 Å root-mean-square deviation (rmsd) among all side chain atoms within 10 Å of the ThDP cofactor. Binding of MBP does not cause large-scale structural rearrangements, as the structure superimposes readily on the previously

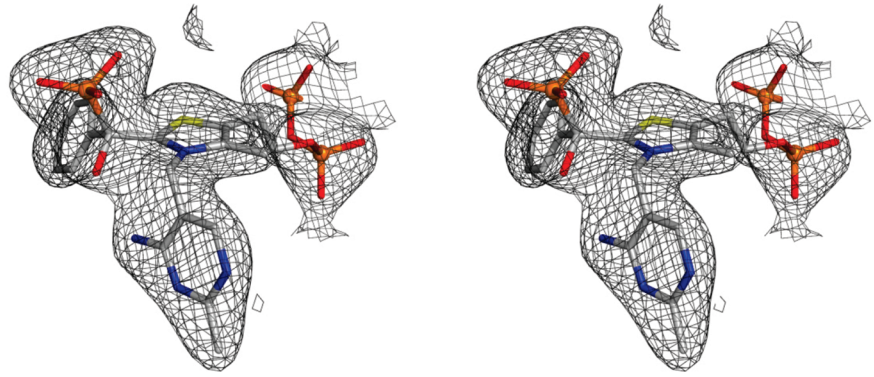

FIGURE 4: Stereoview of the covalent adduct formed between the ThDP cofactor of BAL and the inhibitor MBP, showing the newly formed covalent bond to MBP. Gray mesh represents an electron density map with $2F_o - F_c$ coefficients contoured at 1σ. For clarity, the methyl group of the MBP phosphonoester is not shown (PDB entry 3D7K).

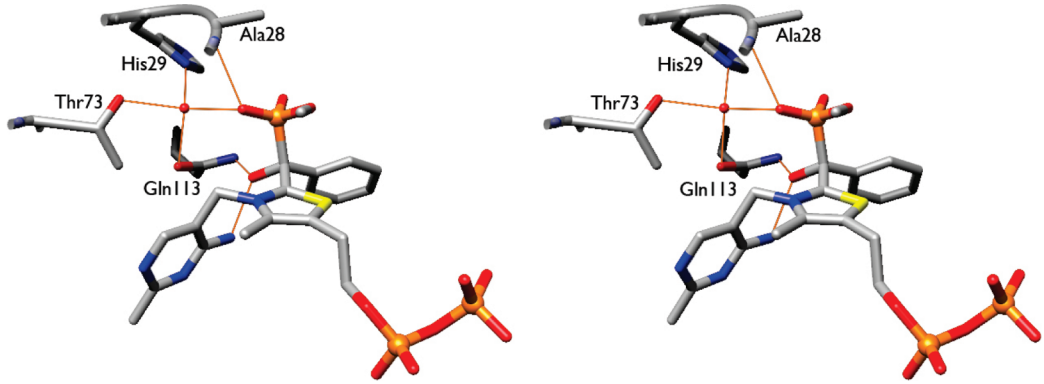

FIGURE 5: Stereoview of the BAL ThDP−MBP adduct, showing the probable hydrogen bonding network of MBP.

reported structure of BAL (PDB entry 2AG0), with an overall α-carbon rmsd of 0.7 Å and an all-atom rmsd of 0.4 Å among side chains within a 10 Å radius of the cofactor. In cocrystallization experiments with MBP and BAL, an omit map indicated positive difference density contiguous with that of the cofactor. Chemically plausible alternate conformations and configurations (including both the *S* and *R* isomers, for example) of reacted and unreacted MBP were placed in the electron density, and the quality of fit was assessed by whether refinement of the model resulted in improved definition of the local electron density map. As shown in Figure 4, modeling the covalent adduct arising from addition of the thiazolium ylide to the carbonyl of MBP gave the best fit to the observed electron density.

Extrapolation from Structural Data. At a spatial resolution of 2.49 Å, uncertainty about heavy atom positions makes assignment of hydrogen bonds somewhat equivocal (*23, 24*). Likely hydrogen bonding interactions between the adduct and the protein that are supported by distance, geometry and chemical considerations are indicated in Figure 5. In addition, identification of water molecules is, to some extent, a matter of interpretation. Water molecules were placed in the active site only when omit maps of the active site show electron density with a clear signal (>4σ). The methyl group of the MBP's monomethyl phosphonoester is not clearly evident in the electron density. This probably arises from heterogeneous distribution in active sites within the crystal. Since a definitive assignment may not be made, the methyl group is assigned at one-third occupancy to a single phosphonate oxygen.

MBP Binding Mode. The phosphonate group of MBP has only two potential hydrogen bonding partners, an active site water and the main chain amide nitrogen of Ala28 of the neighboring subunit (Figure 5). With respect to the carbinol oxygen resulting from thiazolium attack, both distance and geometry are consistent with an intramolecular hydrogen bond with the exocyclic imine (N4′) of the pyrimidinium ring of the cofactor and the amide nitrogen of Gln113. At this resolution, the orientation of the Gln side chain is not fully resolvable, and the oxygen and nitrogen could be reversed. However, available experimental evidence favors the assignment shown, as the CD spectrum confirms the identity of the 1′,4′-imino form of the pyrimidinium ring. In this tautomer, the N4′ lone pair is presented to the carbinol of MBP, fixing the directionality of the hydrogen bond. With regard to binding contacts between BAL and the phenyl ring of MBP, a pocket made up of the side chains of Met421A, Tyr397A, Ala394A, Ala480A, Leu398A, and Leu112B appears responsible, as each of these side chains moves within 5 Å of the phenyl atoms. (Figure 6).

BAL Variants at His29 and Trp163. Kinetic Consequences of the Substitutions. When His29 or Trp163 is substituted with alanine, the activity measured in the presence of 0.50 mM ThDP was 2.7% (H29A) or 92% (W163A), respectively, compared to the activity of wild-type BAL (Figures 7 and 8). The absence of ThDP in the assay medium (in this case the ThDP was supplied by the enzyme only) did not affect the activity of the wild type (98%) or H29A (2.4%) but reduced the W163A BAL activity (56%), indicating that the W163A substitution affects ThDP binding, even though the X-ray structure shows that this residue is 10 Å from the closest ThDP heavy atom and not directly involved in ThDP binding (Figure 10).

The rate of formation of benzoin from benzaldehyde in

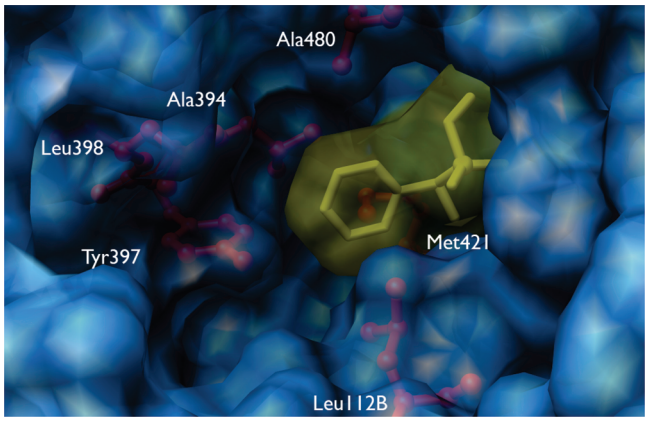

FIGURE 6: Surface rendering of BAL with bound MBP, showing the residues (red) making up the hydrophobic binding pocket for the phenyl ring of the inhibitor (yellow). For clarity, the ThDP cofactor is not shown.

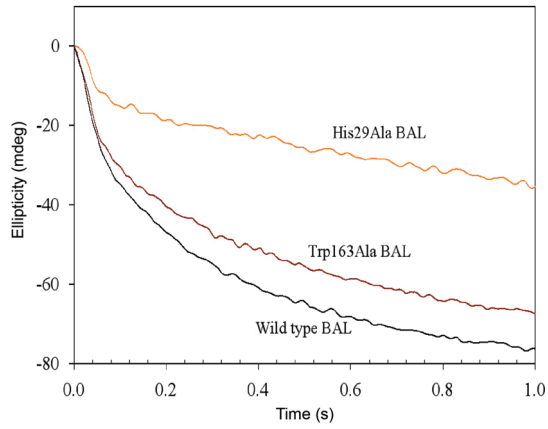

FIGURE 7: Detection of (*R*)-benzoin formation in stopped-flow CD. BAL (2 mg/mL, 33.94 μM) in 50 mM Tris-HCl (pH 8.0) containing 1 mM $MgSO_4$ and 0.20 mM ThDP was mixed with an equal volume of 20 mM benzaldehyde in the same buffer. The reaction was monitored at 313 nm in a 10 mm cell with a slit width of 2 nm for 5 s. Data points were collected every 2.5 ms.

the ligase reaction catalyzed by wild-type, H29A, and W163A BAL was studied by stopped-flow CD. As shown in Figure 7, the reactions all displayed a biphasic rate of formation of (*R*)-benzoin. In the fast phase, H29A was approximately 15 times slower (1.15 ± 0.57 s^{-1}; 0.37 ± 0.01 s^{-1}) than the wild type (16.2 ± 1.85 s^{-1}; 0.62 ± 0.03 s^{-1}), whereas W163A was almost two times slower (7.84 ± 0.53 s^{-1}; 0.46 ± 0.02 s^{-1}). Conversely, in the slower phase, all variants displayed similar rates. Apparently, the H29A substitution affects both the lyase and ligase activities of BAL.

Circular Dichroism Observation of the Interaction of ThDP with the H29A and W163A BAL Variants. The CD spectra of the two BAL variants in the presence of 0.20 mM ThDP indicated the presence of the AP form of ThDP, as in wild-type BAL. The amplitude of the negative CD band at 326 nm was 80% for W163A BAL compared to that of the wild-type enzyme, while only a weak band was detected for H29A BAL (Figure 8A). Further, the CD spectrum of H29A BAL remained unchanged upon addition of 0.10−0.50 mM ThDP (data not shown). By contrast, with W163A BAL, the amplitude of the CD band at 326 nm increased on incremental addition of ThDP (Figure 8B), reaching a maximum ellipticity for a ThDP to W163A subunit molar concentration

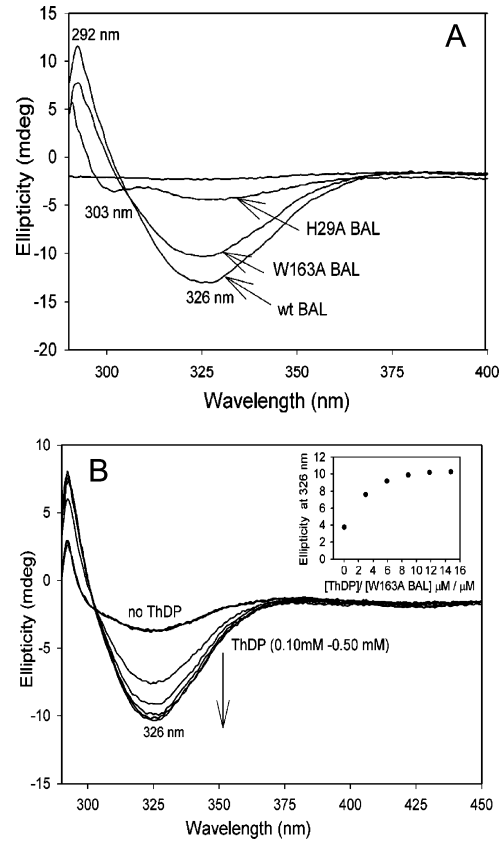

FIGURE 8: Near-UV CD spectra of wild-type BAL and its H29A and W163A active center variants. (A) Comparison of the near-UV CD spectra of wild-type BAL and its H29A and W163A variants (each at a concentration of 2.0 mg/mL, concentration of active centers of 33.9 μM) recorded in 50 mM Tris-HCl (pH 8.0), containing 1 mM $MgSO_4$ and 0.20 mM ThDP. (B) Near-UV CD spectra of W163A BAL recorded in the absence and presence of 0.10−0.50 mM ThDP. The inset shows the dependence of the CD at 326 nm on the ThDP to W163A BAL concentration ratio.

ratio of 16:1 as compared with the 1:1 ratio obtained for the wild type (not presented). Taken together, the data indicate that the W163A substitution on BAL affects ThDP binding. H29A BAL exhibits a much reduced amplitude for the AP form, perhaps due to a shift to the APH^+ form of ThDP, a form which we cannot detect by CD.

Upon addition of MBP, both the H29A and W163A variants developed the positive CD band at 312−314 nm that was seen with the wild-type enzyme in Figure 2. W163A BAL behaved like wild-type BAL ($S_{0.5\ MBP} = 16.4$ μM; $n_H = 2.0$) (data not shown). With the H29A variant, while the intensity of the signal at 314 nm was only 27% of that of the wild type, its affinity for MBP was broadly similar [$S_{0.5\ MBP} = 15.6$ μM; $n_H = 1.95$ (Figure 9 inset)].

DISCUSSION

Mimicking the First Reaction Intermediate with the Substrate Analogue MBP. The monomethyl ester of benzoyl phosphonate (MBP), an analogue of the substrate benzoylformate, has been used in this study to provide insight into the first step of the benzaldehyde lyase reaction. The Kitz−Wilson plot (Figure 1B) shows the kinetics of inhibition by MBP, indicating that while bound in the active centers, MBP does not saturate the enzyme. The steady-state CD experiments (Figure 2) confirmed formation of the 1′,4′-

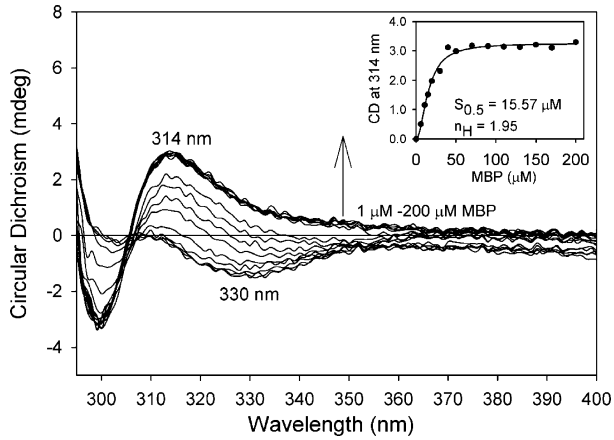

FIGURE 9: Near-UV CD spectra of H29A BAL titrated by MBP. H29A BAL (2 mg/mL, concentration of active centers of 33.9 μM) in 50 mM Tris-HCl (pH 8.0) was titrated with 1−200 mM MBP. The inset shows the dependence of the amplitude of the CD band at 314 nm on the concentration of MBP. The CD at 314 nm was obtained by the subtraction of the CD at 314 nm in the absence of MBP.

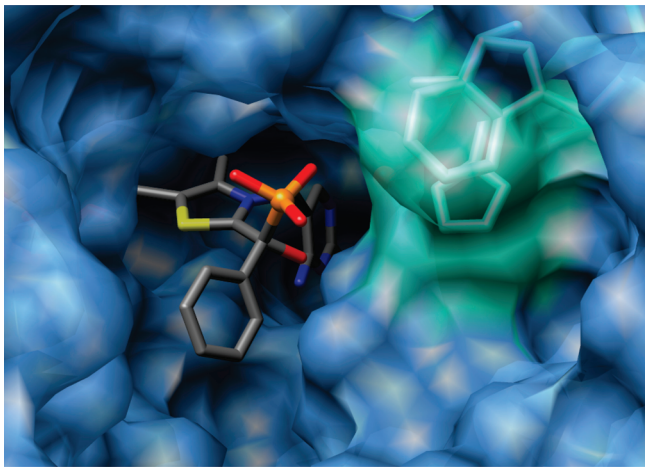

FIGURE 10: View of the active site cleft showing the importance of Trp163 and His29 (green) in making up the active site. In addition, the relative disposition of the Trp163 and His29 side chains may represent a geometry consistent with an energetically favorable stacking interaction. For clarity, the MBP phosphonate methyl group is not shown.

imino tautomer of the covalent adduct between ThDP and MBP, and time-resolved CD experiments (Figure 3) determined the rate of adduct formation. Aliphatic congeners of MBP have been used as mechanism-based inhibitors of ThDP-dependent enzymes acting on pyruvate (*4–7, 33–35*). The products of these reactions are thought to be stable mimics for the complex that results from reaction between ThDP and pyruvate. The free acid, benzoylphosphonate, was found to inhibit the ThDP-dependent benzoylformate decarboxylase, but surprisingly, the inhibition resulted from phosphorylation of an active site serine rather than from formation of a stable adduct (*36*). The kinetic evidence and CD spectroscopic evidence both suggest that MBP binds in the active centers of BAL and forms a covalent intermediate, C2α-phosphonomandelylThDP, an analogue of MThDP, the pre-decarboxylation intermediate derived from benzoylformate (Scheme 2). This was deduced from the positive CD band produced at 312−314 nm, which reflects the presence of the 1′,4′-iminopyrimidine form of PMThDP (Figure 2). This is characteristic of tetrahedral substitution at the C2α atom of ThDP and has now been observed on six ThDP-dependent enzymes.

Crystal Structure of the Covalent Adduct of MBP. To attempt direct observation of the steady-state covalent complex, BAL was incubated with MBP and crystallized, following a published protocol for crystallization of native BAL (*14*). The structure was determined to a spatial resolution of 2.49 Å and represents the first reported structure of BAL with a substrate analogue bound in the active site (Table 1). The covalent nature of the adduct formed between MBP and the ThDP cofactor is clear from an examination of the active site electron density (Figure 4).

The first step of catalysis, which the cofactor−inhibitor complex in this structure is thought to mimic, is not accompanied by any large-scale movements of either BAL or ThDP (rmsd of 0.7 Å). Thus, our study confirms the prevailing notion that the enzyme positions the cofactor for catalysis prior to substrate binding (*2, 6, 37–39*). In this respect, BAL is similar to the other structurally characterized members of the family of ThDP-dependent enzymes. Indeed, comparison to pyruvate dehydrogenase (PDHc) and pyruvate oxidase (POX), both of which were recently characterized after irreversible inactivation with a phosphonate inhibitor, reveals very strong conservation of cofactor geometry (*33, 35*).

Binding Mode of MBP. Given that this is the first structure of a substrate analogue in the BAL active site, some interpretation of the binding mode is warranted, in light of known mechanistic aspects of the reaction. Salient details of the binding are shown in Figures 5 and 6. A fundamental mechanistic question is the identity of active site acids and bases responsible for the transfer of a proton to and from the substrate. Surprisingly, the only credible candidate for general acid−base catalysis is His29. Thr481 of the second subunit is a conceivable proton donor, but its hydroxyl group is oriented away from the substrate in favor of a hydrogen bonding opportunity with the backbone of Trp478. When a rotamer of Thr481 more favorable to substrate interaction was examined, refinement showed that the fit of this alternate rotamer to the electron density was very poor. The closest approach of the ϵ-nitrogen of His29 to a phosphate oxygen is 4.3 Å, implying that His29 would be too distant to have a direct acid−base interaction with the alcohol of BAL's benzoin substrate. However, we cannot rule out the possibility of structural rearrangement upon binding the natural substrate, benzoin, that would bring His29 within range.

Interaction with Iminium N4′ of ThDP. An interesting feature of thiamin-dependent catalysis is the potential for an intramolecular hydrogen bond to the carbinol oxygen formed by addition of the thiazolium ylide to the substrate carbonyl. At present, data are available from the structures of pyruvate dehydrogenase (PDHc) and pyruvate oxidase (POX) (*33, 35*). With acyl phosphonates, thiazolium attack results in a methyl carbinol, but at the spatial resolution of these structures, the distinction between a methyl and hydroxyl group is not clear from the electron density. Therefore, the assignment was made on chemical grounds. The lobe of electron density in position to make a hydrogen bond with the exocyclic amine of the ThDP pyrimidinium nitrogen was presumed to be the hydroxyl group (*33, 35*). This assignment is undoubtedly reasonable, and evidence from this structure would seem to confirm it. Addition to the benzoyl phosphonate results in a phenyl carbinol, and

the hydroxyl and phenyl group are readily distinguished at a resolution of 2.49 Å. It is clear from this structure both that the depicted carbinol accounts more thoroughly for the observed omit map density than its enantiomer and that the carbinol oxygen is well-positioned to make a hydrogen bond with ThDP (Figures 4 and 5). The importance of N4′ to catalysis in ThDP-dependent enzymes is further emphasized by a recent study which suggests that oxidation of this functionality to the oxime abrogates activity in pyruvate-ferredoxin oxidoreductase (*40*).

The structure also permits analysis of how the enzyme enforces stereoelectronic constraints to influence the course of the reaction (*41*). To explain the perpendicular alignment of the C−P bond with regard to the thiazolium ring, the hypothesis originally proposed by Dunathan may be invoked (*42*). The observed configuration aligns the C−C bond to be broken during decarboxylation with the π system of the thiazolium. In this way, the developing p orbital is geometrically disposed to achieve maximal overlap with the thiazolium π orbitals, thus lowering the barrier to bond breaking. This mechanism has been proposed for ThDP-dependent catalysis of decarboxylation (*43–45*). This structure offers additional experimental corroboration of this model.

Effect of the H29A and W163A Substitutions on ThDP Binding, Catalysis, and Tautomerization. Consistent with its position in the active site (Figure 5) and its possible role as an acid−base catalyst, the H29A variant had been shown to exhibit a 10-fold reduction in value of k_{cat}, although its K_m value for benzoin was largely unaffected (*15*). Trp163 is located above His29, and it could potentially be involved in a stacking interaction that could modulate the activity of His29 (Figure 10). In addition, it had been suggested that the negative CD band at 326 nm in other ThDP enzymes was the result of an interaction with Trp and the thiazolium ring of ThDP (*46*). To explore both these possibilities, the H29A and W163A variants were prepared.

Confirming those of the early study (*13*), our results show that the H29A substitution decreases both the lyase and ligase activities of BAL. Conversely, the W163A substitution affects mostly the affinity of ThDP for BAL. The H29A substituted enzyme shows a very weak negative band at 326 nm in the near-UV CD spectra indicating one or both of the following: (a) the proper orientation of ThDP in the active center is affected, or (b) the pK_a for conversion of APH^+ to the AP form is shifted. In other words, if the pK_a increases, a smaller fraction of the AP form would be detected at the same pH (Scheme 1, left, and ref *8* for this pK_a).

If His29 is indeed positively charged in the wild-type enzyme, this would tend to favor the AP form over the APH^+ form. Now, conversion of His29 to Ala removes the positive charge and shifts the equilibrium to the APH^+ form (increasing the pK_a compared to that of the wild type), which is evident from CD data, explaining (a) a small band for the AP tautomer with ThDP, (b) a small band for the IP band with MBP, and (c) the lower activity in both lyase and ligase directions.

Upon addition of MBP, both variants showed formation of the MBThDP covalent intermediate in its 1′,4′-iminopyrimidine tautomeric form. The W163A variant behaves like wild-type BAL, but the H29A variant displays only a weak CD band in this region, again probably consistent with one of the explanations in the earlier paragraphs.

Since Trp163 is distal to the ThDP binding site [~10 Å (Figure 10)], it may be that both the activity and ThDP binding are affected by His29, raising the possibility of two distinct roles of His29. First, replacement of His29 with alanine has a marked effect on the activity, confirming the importance suggested by its proximity to an important structural water molecule (Figure 5). Second, perhaps it plays a role in preventing ThDP from dissociating from the protein indirectly by its interaction with Trp163. It is tempting to speculate that the tryptophan side chainstacked as it is almost within van der Waals contact (3.5 Å) of His29, promotes protonation of the imidazole in the absence of substrate. Cation−π interactions between tryptophan and imidazolium have been observed in numerous systems (*47–49*).

If His29 is also too distant to interact with the substrate, why does its conversion to alanine have such a marked effect on activity? The structure presented here, like the structure of BAL without MBP bound, strongly suggests that His29 is critical in positioning the active site water rather than interacting directly with the substrate. More importantly, detailed analysis of the functional data shows that the substitution does not alter the enzyme's K_m value, but it does result in a roughly 10-fold decrease in k_{cat} (*15*). These data were interpreted to support the idea that proton transfer in the BAL active site is mediated by water. These results, showing that H29A substitution compromises the enzyme's ability to maintain the catalytically active cofactor tautomer, may offer a different explanation for its effects on enzyme activity. However, short of unanticipated structural rearrangement, general acid−base catalysis is still the most plausible explanation for proton shuttling in the BAL active site.

REFERENCES

1. Knoll, M., Muller, M., Pleiss, J., and Pohl, M. (2006) Factors mediating activity, selectivity, and substrate specificity for the thiamin diphosphate-dependent enzymes benzaldehyde lyase and benzoylformate decarboxylase. *ChemBioChem 7*, 1928–1934.
2. Pohl, M., Sprenger, G. A., and Muller, M. (2004) A new perspective on thiamine catalysis. *Curr. Opin. Biotechnol. 15*, 335–342.
3. Chakraborty, S., Nemeria, N., Yep, A., McLeish, M. J., Kenyon, G. L., and Jordan, F. (2008) Mechanism of benzaldehyde lyase studied via thiamin diphosphate-bound intermediates and kinetic isotope effects. *Biochemistry 47*, 3800–3809.
4. Nemeria, N., Baykal, A., Joseph, E., Zhang, S., Yan, Y., Furey, W., and Jordan, F. (2004) Tetrahedral intermediates in thiamin diphosphate-dependent decarboxylations exist as a 1′,4′-imino tautomeric form of the coenzyme, unlike the Michaelis complex or the free coenzyme. *Biochemistry 43*, 6565–6575.
5. Nemeria, N., Korotchkina, L., McLeish, M. J., Kenyon, G. L., Patel, M. S., and Jordan, F. (2007) Elucidation of the chemistry of enzyme-bound thiamin diphosphate prior to substrate binding: Defining internal equilibria among tautomeric and ionization states. *Biochemistry 46*, 10739–10744.
6. Jordan, F. (2003) Current mechanistic understanding of thiamin diphosphate-dependent enzymatic reactions. *Nat. Prod. Rep. 20*, 184–201.
7. Nemeria, N., Chakraborty, S., Baykal, A., Korotchkina, L. G., Patel, M. S., and Jordan, F. (2007) The 1′,4′-iminopyrimidine tautomer of thiamin diphosphate is poised for catalysis in asymmetric active centers on enzymes. *Proc. Natl. Acad. Sci. U.S.A. 104*, 78–82.
8. Jordan, F., and Mariam, Y. H. (1978) N1′-Methylthiaminium diiodide: Model study on effect of a coenzyme bound positive charge on reaction-mechanisms requiring thiamin pyrophosphate. *J. Am. Chem. Soc. 100*, 2534–2541.

9. Jordan, F., Zhang, Z., and Sergienko, E. (2002) Spectroscopic evidence for participation of the 1′,4′-imino tautomer of thiamin diphosphate in catalysis by yeast pyruvate decarboxylase. *Bioorg. Chem. 30*, 188–198.
10. Nemeria, N., Tittmann, K., Joseph, E., Zhou, L., VazquezColl, M. B., Arjunan, P., Hubner, G., Furey, W., and Jordan, F. (2005) Glutamate 636 of the *Escherichia coli* pyruvate dehydrogenase-E1 participates in active center communication and behaves as an engineered acetolactate synthase with unusual stereoselectivity. *J. Biol. Chem. 280*, 21473–21482.
11. Schellenberger, A. (1998) Sixty years of thiamin diphosphate biochemistry. *Biochim. Biophys. Acta 1385*, 177–186.
12. Baykal, A. T., Kakalis, L., and Jordan, F. (2006) Electronic and nuclear magnetic resonance spectroscopic features of the 1′,4′-iminopyrimidine tautomeric form of thiamin diphosphate, a novel intermediate on enzymes requiring this coenzyme. *Biochemistry 45*, 7522–7528.
13. Maraite, A., Schmidt, T., AnsorgeSchumacher, M. B., Brzozowski, A. M., and Grogan, G. (2007) Structure of the ThDP-dependent enzyme benzaldehyde lyase refined to 1.65 Å resolution. *Acta Crystallogr. D63*, 546–548.
14. Mosbacher, T. G., Mueller, M., and Schulz, G. E. (2005) Structure and mechanism of the ThDP-dependent benzaldehyde lyase from *Pseudomonas fluorescens*. *FEBS J. 272*, 6067–6076.
15. Kneen, M. M., Pogozheva, I. D., Kenyon, G. L., and McLeish, M. J. (2005) Exploring the active site of benzaldehyde lyase by modeling and mutagenesis. *Biochim. Biophys. Acta 1753*, 263–271.
16. Karaman, R., Goldblum, A., Breuer, E., and Leader, H. (1989) Acylphosphonic acids and methyl hydrogen acylphosphonates: Physical and chemical properties and theoretical calculations. *J. Chem. Soc., Perkin Trans. 1*, 765–774.
17. Bailey, S. (1994) The CCP4 suite: Programs for protein crystallography. *Acta Crystallogr. D50*, 760–763.
18. Otwinowski, Z., and Minor, W. (1997) Processing of X-ray diffraction data collected in oscillation mode. *Methods Enzymol. 276*, 307–326.
19. Vagin, A., and Teplyakov, A. (1997) MOLREP: An automated program for molecular replacement. *J. Appl. Crystallogr. 30*, 1022–1025.
20. McCoy, A. J., Grosse-Kunstleve, R. W., Adams, P. D., Winn, M. D., Storoni, L. C., and Read, R. J. (2007) Phaser crystallographic software. *J. Appl. Crystallogr. 40*, 658–674.
21. Murshudov, G. N., Vagin, A. A., and Dodson, E. J. (1997) Refinement of macromolecular structures by the maximum-likelihood method. *Acta Crystallogr. D53*, 240–255.
22. Emsley, P., and Cowtan, K. (2004) Coot: Model-building tools for molecular graphics. *Acta Crystallogr. D60*, 2126–2132.
23. Acharya, K. R., and Lloyd, M. D. (2005) The advantages and limitations of protein crystal structures. *Trends Pharmacol. Sci. 26*, 10–14.
24. Kleywegt, G. J. (2000) Validation of protein crystal structures. *Acta Crystallogr. D56*, 249–265.
25. Potterton, E., Briggs, P., Turkenburg, M., and Dodson, E. (2003) A graphical user interface to the CCP4 program suite. *Acta Crystallogr. D59*, 1131–1137.
26. Schuttelkopf, A. W., and van Aalten, D. M. F. (2004) PRODRG: A tool for high-throughput crystallography of protein-ligand complexes. *Acta Crystallogr. D60*, 1355–1363.
27. Hooft, R. W., Vriend, G., Sander, C., and Abola, E. E. (1996) Errors in protein structures. *Nature 381*, 272.
28. Laskowski, R. A., Macarthur, M. W., Moss, D. S., and Thornton, J. M. (1993) PROCHECK: A program to check the stereochemical quality of protein structures. *J. Appl. Crystallogr. 26*, 283–291.
29. Vaguine, A. A., Richelle, J., and Wodak, S. J. (1999) SFCHECK: A unified set of procedures for evaluating the quality of macromolecular structure-factor data and their agreement with the atomic model. *Acta Crystallogr. D55*, 191–205.
30. Kitz, R., and Wilson, I. B. (1962) Esters of methanesulfonic acid as irreversible inhibitors of acetylcholinesterase. *J. Biol. Chem. 237*, 3245–3249.
31. Baykal, A., Chakraborty, S., Dodoo, A., and Jordan, F. (2006) Synthesis with good enantiomeric excess of both enantiomers of α-ketols and acetolactates by two thiamin diphosphate-dependent decarboxylases. *Bioorg. Chem. 34*, 380–393.
32. Janzen, E., Muller, M., Kolter-Jung, D., Kneen, M. M., McLeish, M. J., and Pohl, M. (2006) Characterization of benzaldehyde lyase from *Pseudomonas fluorescens*: A versatile enzyme for asymmetric C-C bond formation. *Bioorg. Chem. 34*, 345–361.
33. Arjunan, P., Sax, M., Brunskill, A., Chandrasekhar, K., Nemeria, N., Zhang, S., Jordan, F., and Furey, W. (2006) A thiamin-bound, pre-decarboxylation reaction intermediate analogue in the pyruvate dehydrogenase E1 subunit induces large scale disorder-to-order transformations in the enzyme and reveals novel structural features in the covalently bound adduct. *J. Biol. Chem. 281*, 15296–15303.
34. Jordan, F., and Nemeria, N. S. (2005) Experimental observation of thiamin diphosphate-bound intermediates on enzymes and mechanistic information derived from these observations. *Bioorg. Chem. 33*, 190–215.
35. Wille, G., Meyer, D., Steinmetz, A., Hinze, E., Golbik, R., and Tittmann, K. (2006) The catalytic cycle of a thiamin diphosphate enzyme examined by cryocrystallography. *Nat. Chem. Biol. 2*, 324–328.
36. Bera, A. K., Polovnikova, L. S., Roestamadji, J., Widlanski, T. S., Kenyon, G. L., McLeish, M. J., and Hasson, M. S. (2007) Mechanism-based inactivation of benzoylformate decarboxylase, a thiamin diphosphate-dependent enzyme. *J. Am. Chem. Soc. 129*, 4120–4121.
37. Frank, R. A. W., Leeper, F. J., and Luisi, B. F. (2007) Structure, mechanism and catalytic duality of thiamine-dependent enzymes. *Cell. Mol. Life Sci. 64*, 892–905.
38. Lie, M. A., Celik, L., Jorgensen, K. A., and Schiott, B. (2005) Cofactor activation and substrate binding in pyruvate decarboxylase. Insights into the reaction mechanism from molecular dynamics simulations. *Biochemistry 44*, 14792–14806.
39. Malandrinos, G., Louloudi, M., and Hadjiliadis, N. (2006) Thiamine models and perspectives on the mechanism of action of thiamine-dependent enzymes. *Chem. Soc. Rev. 35*, 684–692.
40. Cavazza, C., Contreras-Martel, C., Pieulle, L., Chabriere, E., Hatchikian, E. C., and Fontecilla-Camps, J. C. (2006) Flexibility of thiamine diphosphate revealed by kinetic crystallographic studies of the reaction of pyruvate-ferredoxin oxidoreductase with pyruvate. *Structure 14*, 217–224.
41. Eliot, A. C., and Kirsch, J. F. (2003) Avoiding the road less traveled: How the topology of enzyme-substrate complexes can dictate product selection. *Acc. Chem. Res. 36*, 757–765.
42. Dunathan, H. C. (1966) Conformation and reaction specificity in pyridoxal phosphate enzymes. *Proc. Natl. Acad. Sci. U.S.A. 55*, 712–716.
43. Hoskins, A. A., Morar, M., Kappock, T. J., Mathews, I. I., Zaugg, J. B., Barder, T. E., Peng, P., Okamoto, A., Ealick, S. E., and Stubbe, J. (2007) N-5-CAIR mutase: Role of a CO_2 binding site and substrate movement in catalysis. *Biochemistry 46*, 2842–2855.
44. Hu, Q., and Kluger, R. (2004) Fragmentation of the conjugate base of 2-(1-hydroxybenzyl)thiamin: Does benzoylformate decarboxylase prevent orbital overlap to avoid it? *J. Am. Chem. Soc. 126*, 68–69.
45. Wang, J. Y., Dong, H., Li, S. H., and He, H. W. (2005) Theoretical study toward understanding the catalytic mechanism of pyruvate decarboxylase. *J. Phys. Chem. B 109*, 18664–18672.
46. Kochetov, G. A., and Usmanov, R. A. (1970) Charge transfer interactions in transketoloase-thiamine pyrophosphpate complex. *Biochem. Biophys. Res. Commun. 41*, 1134–1140.
47. Fernandez-Recio, J., Vazquez, A., Civera, C., Sevilla, P., and Sancho, J. (1997) The tryptophan/histidine interaction in α-helices. *J. Mol. Biol. 267*, 184–197.
48. Okada, A., Miura, T., and Takeuchi, H. (2001) Protonation of histidine and histidine-tryptophan interaction in the activation of the M2 ion channel from influenza a virus. *Biochemistry 40*, 6053–6060.
49. Takeuchi, H., Okada, A., and Miura, T. (2003) Roles of the histidine and tryptophan side chains in the M2 proton channel from influenza A virus. *FEBS Lett. 552*, 35–38.

BI8004413